

This discussion paper is/has been under review for the journal Atmospheric Chemistry and Physics (ACP). Please refer to the corresponding final paper in ACP if available.

The MIPAS HOCl climatology

**T. von Clarmann¹, B. Funke², N. Glatthor¹, S. Kellmann¹, M. Kiefer¹, O. Kirner³,
B.-M. Sinnhuber¹, and G. P. Stiller¹**

¹Karlsruhe Institute of Technology, Institute for Meteorology and Climate Research, Karlsruhe, Germany

²Instituto de Astrofísica de Andalucía, CSIC, Granada, Spain

³Karlsruhe Institute of Technology, Steinbuch Centre for Computing, Karlsruhe, Germany

Received: 1 June 2011 – Accepted: 2 July 2011 – Published: 22 July 2011

Correspondence to: T. von Clarmann (thomas.clarmann@kit.edu)

Published by Copernicus Publications on behalf of the European Geosciences Union.

The MIPAS HOCl climatology

T. von Clarmann et al.

Title Page

Abstract

Introduction

Conclusions

References

Tables

Figures

◀

▶

◀

▶

Back

Close

Full Screen / Esc

Printer-friendly Version

Interactive Discussion



Abstract

Monthly zonal mean HOCl measurements by the Michelson Interferometer for Passive Atmospheric Sounding (MIPAS) are presented for the episode from June 2002 to March 2004. Highest molar mixing ratios are found at pressure levels between 6 and 2 hPa, whereby largest mixing ratios occasionally exceed 200 ppt. The mixing ratio maximum is generally at lower altitudes in the summer hemisphere than in the winter hemisphere except for chlorine activation conditions in polar vortices, where enhanced HOCl abundances are also found in the lower stratosphere. During nighttime the maximum is found at higher altitudes than during daytime. Particularly low values are found in subpolar regions in the winter hemisphere, coinciding with the mixing barrier formed by the polar vortex boundary. The Antarctic polar winter HOCl distribution in 2002, the year of the split of the southern polar vortex, resembles northern polar winters rather than other southern polar winters. Increased HOCl amounts in response to the so-called Halloween solar proton event in autumn 2003 affect the representativeness of data recorded during this particular episode. Calculations with the EMAC model reproduce the structure of the measured HOCl distribution but predict approximately 40% less HOCl except during polar night in the mid-stratosphere where calculated HOCl mixing ratios exceed observed ones.

1 Introduction

HOCl is a short-lived reservoir of ClO_x and HO_x and thus links stratospheric chlorine and odd hydrogen chemistry. The HOCl catalytic cycle is an important mechanism for midlatitude stratospheric ozone loss (Solomon et al., 1986). In polar vortices HOCl has heterogeneous sources and sinks and thus can contribute to the polar chlorine chemistry (Hanson and Ravishankara, 1992; Abbatt and Molina, 1992; Crutzen et al., 1992; Prather, 1992; von Clarmann et al., 2009a). It also serves as indicator for perturbed HO_x chemistry (von Clarmann et al., 2005). There exist occasional HOCl

ACPD

11, 20793–20822, 2011

The MIPAS HOCl climatology

T. von Clarmann et al.

Title Page

Abstract

Introduction

Conclusions

References

Tables

Figures

◀

▶

◀

▶

Back

Close

Full Screen / Esc

Printer-friendly Version

Interactive Discussion



measurements from balloon-, space-, and airborne infrared solar absorption experiments (Larsen et al., 1985; Toon et al., 1992; Raper et al., 1987), balloon-borne far infrared limb emission (Chance et al., 1989; Traub et al., 1990; Johnson et al., 1995), as well as balloon-borne infrared limb emission (von Clarmann et al., 1997) measurements. MIPAS (Michelson Interferometer for Passive Atmospheric Sounding) provided the first global HOCl data set (von Clarmann et al., 2006). Further global HOCl measurements have been provided by the Microwave Limb Sounder (MLS) (Cofield and Stek, 2006) and JEM/SMILES (Kasai et al., 2009).

Large discrepancies between measured and modeled HOCl abundancies were found by Kovalenko et al. (2007), suggesting that reaction rate coefficients for HOCl formation from ClO and HO₂ as published by Stimpfle et al. (1979) might be more appropriate than the current JPL recommendation (Sander et al., 2006). This has been confirmed by von Clarmann et al. (2009a).

In this paper we present the first climatology of global altitude-resolved HOCl measurements, covering a full annual cycle, based on MIPAS measurements and compare these data to model calculations based on different rate coefficients of HOCl formation.

2 MIPAS HOCl data

MIPAS is a Fourier transform limb emission spectrometer operated to measure vertical profiles of temperature and mixing ratios of many trace species (Fischer et al., 2008). MIPAS is one of three atmospheric chemistry related instruments on the Envisat research satellite. Envisat has been launched in a sun-synchronous polar orbit of about 800 km altitude, 98.55° inclination, orbital period of 100.6 min, and equator crossing at approximately 10:00 LT (local time). In its original nominal measurement mode MIPAS recorded one set of 17 limb measurements at tangent altitudes from 6 to 68 km per 76.5 s, i.e. per 510 km ground track at a spectral resolution of 0.05 cm⁻¹ apodized. After failure of the interferometer slide, regular operation was interrupted in 2004. Since 2005 MIPAS is operational again, however at reduced spectral but improved spatial

The MIPAS HOCl climatology

T. von Clarmann et al.

Title Page

Abstract

Introduction

Conclusions

References

Tables

Figures

◀

▶

◀

▶

Back

Close

Full Screen / Esc

Printer-friendly Version

Interactive Discussion



5 resolution. While for many trace species the change of operation mode turned out to be advantageous in terms of precision, altitude-, and along-track horizontal resolution (Chauhan et al., 2009; von Clarmann et al., 2009b), HOCl could not yet successfully be retrieved from these reduced resolution measurements, because its lines could not be well enough resolved among the much stronger lines of interfering species.

HOCl is retrieved from MIPAS spectra using the IMK/IAA scientific MIPAS processor (von Clarmann et al., 2003) by constrained least-squares fitting of simulated to measured spectral radiances. Details of the retrieval settings are discussed in von Clarmann et al. (2006). A Tikhonov-type first order finite differences constraint, modified to allow an altitude-dependent choice of the strength of the regularization (Steck and von Clarmann, 2001) has been chosen in order to avoid biasing of retrievals towards the a priori information. The measurement error was found to be largely dominated by measurement noise. The precision of a single profile measurement is estimated at 30 to 80 ppt, i.e. about 25 % of the peak molar mixing ratio. The altitude resolution is about 9 km, due to the strong smoothing constraint needed to obtain stable retrievals at low signal/noise ratio. MIPAS averaging kernels are well-behaved in an altitude-range between about 20 and 45 km, in a sense that they are approximately symmetric around their nominal altitudes (Fig. 1). In this altitude region the MIPAS HOCl profiles can be regarded as a smoothed version of the true HOCl profiles. At altitudes above 45 km and below 20 km the sensitivity of the MIPAS HOCl retrievals is largely reduced, and the asymmetric averaging kernels shift information from these altitudes into the altitude range where MIPAS is sensitive. In the presence of HOCl at these altitudes, application of the MIPAS averaging kernels is thus particularly important to make high-resolution model results comparable to MIPAS measurements (cf., e.g. Jackman et al., 2008). Since the MIPAS a priori profiles are zero throughout, this transformation reduces to

$$\mathbf{x}_{\text{degraded}} = \mathbf{A} \mathbf{x}_{\text{fine}}, \quad (1)$$

where \mathbf{x}_{fine} is the high-resolution HOCl profile, $\mathbf{x}_{\text{degraded}}$ is the degraded profile which should be used for the comparison, and \mathbf{A} is the MIPAS averaging kernel matrix. MIPAS averaging kernels have the same structure and characteristics for all seasons

The MIPAS HOCl climatology

T. von Clarmann et al.

[Title Page](#)[Abstract](#)[Introduction](#)[Conclusions](#)[References](#)[Tables](#)[Figures](#)[◀](#)[▶](#)[◀](#)[▶](#)[Back](#)[Close](#)[Full Screen / Esc](#)[Printer-friendly Version](#)[Interactive Discussion](#)

and latitude bands; small to moderate differences reflect the seasonal and latitudinal temperature variation. No substantial differences between daytime and nighttime averaging kernels are observed. This is because at relevant altitudes the atmosphere is rather transparent, leading to linear radiative transfer and thus independence of the Jacobians (and thus averaging kernels) from the actual mixing ratio of HOCl.

MIPAS results were found in good agreement with trend-corrected earlier measurements reported by Chance et al. (1989, 1996). The most recent version of MIPAS HOCl data is V30.HOCl.4. Improvements with respect to previous data versions are obtained by consideration of horizontal temperature gradients, stronger regularization of N₂O profiles which are jointly fitted, a finer monochromatic wavenumber grid used in the radiative transfer calculation, a larger number of pencil beams for radiance integration over the instantaneous field of view, and some updates of spectroscopic data of gases used in the radiative transfer calculations.

3 Method

MIPAS HOCl climatologies have been prepared in compliance with the methodical and data format requirements of the SPARC (Stratospheric Processes and their Role in Climate) Data Initiative (Hegglin and Tegtmeier, 2011). The climatology consists of zonal monthly mean fields of HOCl molar mixing ratios and their standard deviations and sample sizes. In order to account for the diurnal variability of HOCl, separate mean fields are provided for a.m. and p.m. measurements. The altitude grid is 300, 250, 200, 170, 150, 130, 115, 100, 90, 80, 70, 50, 30, 20, 15, 10, 7, 5, 3, 2, 1.5, 1.0, 0.7, 0.5, 0.3, 0.2, 0.15, 0.1 hPa, and the centers of the equidistant latitude bins are -87.5° , -82.5° , ..., 82.5° , 87.5° . Each profile was first interpolated to the pressure grid using MIPAS pressure and temperature profiles (von Clarmann et al., 2006) and then averaged. Since MIPAS measured one profile each 510 km ground track distance from a polar orbit, only one or two profiles per orbit segment fall within a latitude bin. Since the measurement sequence is re-initialized at a fixed latitude during each orbit, this

The MIPAS HOCl climatology

T. von Clarmann et al.

Title Page

Abstract

Introduction

Conclusions

References

Tables

Figures

◀

▶

◀

▶

Back

Close

Full Screen / Esc

Printer-friendly Version

Interactive Discussion



leads to a systematic sampling bias, i.e. the MIPAS measurement does not generally represent the nominal central latitude of the latitude bin. In order to avoid related artefacts, it has been decided to linearly interpolate the MIPAS measurements to the nominal latitudes. Standard deviations and the number of measurements are provided along with the molar mixing ratios. The number of profile measurements per monthly zonal mean and time of the day (a.m. or p.m.) was typically between 400 and 800. Since the interpolation of these quantities to the nominal latitude grid is not a trivial task, particularly if both measurement errors and natural variability contribute to the variance, related operations are discussed in detail in Appendix A.

4 Model calculations

In order to assess how well HOCl chemistry is understood on a global scale, MIPAS climatologies are compared to model calculations of the Chemistry Climate Model (CCM) EMAC (ECHAM5/MESSy Atmospheric Chemistry model) (Jöckel et al., 2006). EMAC has been developed at the Max-Planck-Institute for Chemistry in Mainz and is a combination of the general circulation model ECHAM5 (Roeckner et al., 2006) and different submodels such as the chemistry submodel MECCA1 (Sander et al., 2005) combined through the Modular Earth Submodel System MESSy (Jöckel et al., 2005).

For this study data from a simulation from 1994 to 2011 with EMAC Version 1.10 are used. The simulation was performed with horizontal resolution T42 ($2.8^\circ \times 2.8^\circ$) and with 39 layers, covering the atmosphere from the surface up to 0.01 hPa (≈ 80 km). A Newtonian relaxation technique of the prognostic variables temperature, vorticity, divergence and the surface pressure above the boundary layer and below 10 hPa towards ECMWF operational analysis data has been applied, in order to nudge the model dynamics towards the observed meteorology. The boundary conditions for greenhouse gases are from the IPCC-A1B scenario (IPCC, 2001) adapted to observations from the AGAGE database (Prinn et al., 2001) and for halogenated hydrocarbons from the WMO-Ab scenario (World Meteorological Organization, 2007).

The MIPAS HOCl climatology

T. von Clarmann et al.

Title Page

Abstract

Introduction

Conclusions

References

Tables

Figures

◀

▶

◀

▶

Back

Close

Full Screen / Esc

Printer-friendly Version

Interactive Discussion



**The MIPAS HOCl
climatology**

T. von Clarmann et al.

[Title Page](#)[Abstract](#)[Introduction](#)[Conclusions](#)[References](#)[Tables](#)[Figures](#)[◀](#)[▶](#)[◀](#)[▶](#)[Back](#)[Close](#)[Full Screen / Esc](#)[Printer-friendly Version](#)[Interactive Discussion](#)

The simulation includes a comprehensive atmospheric chemistry setup for the troposphere, the stratosphere and the lower mesosphere. The applied submodels are the same as in the simulations in Kirner (2008). In particular we used a new parameterisation of polar stratospheric clouds based on the efficient growth and sedimentation of NAT-particles in the submodel PSC (Kirner et al., 2011).

Modeled HOCl fields of the 15th of the respective month, sampled at the respective local time (10:00 a.m./10:00 p.m.) are smoothed by the MIPAS averaging kernels and presented for comparison.

5 Twenty-two months of HOCl observations

MIPAS HOCl observations are available from June 2002 to March 2004. The typical features are: The pressure level of maximal mixing ratio varies between 6 and 2 hPa (appr. 35–43 km, respectively). Largest mixing ratios occasionally exceed 200 ppt. The altitude of largest mixing ratios is generally lower in the summer hemisphere than in the winter hemisphere (Fig. 2), except sometimes for polar vortices.

During nighttime the maximum is found at higher altitudes than during daytime (Fig. 3). The approximate altitude (ca. 39 km or 3 hPa during nighttime) and the upward shift of the maximum by about 5 km during nighttime are consistent with the profiles and their diurnal variation found by Chance et al. (1989, 1996) who measured HOCl in the far infrared spectral region from a balloon-borne platform. This shift in altitude of the maximum seems to be more pronounced at lower latitudes than at higher latitudes, leading to quite a flat distribution of the peak altitude over latitude during nighttime contrasting to a slightly more banana-shaped distribution during daytime.

The representation of the data as a timeseries (Fig. 4) shows a semiannual oscillation of the peak mixing ratios in the tropics (equatorward of 25°) with a peak to peak variation of of about 30 ppt. Largest abundances are found in July/August and in January/February.

**The MIPAS HOCl
climatology**

T. von Clarmann et al.

[Title Page](#)[Abstract](#)[Introduction](#)[Conclusions](#)[References](#)[Tables](#)[Figures](#)[◀](#)[▶](#)[◀](#)[▶](#)[Back](#)[Close](#)[Full Screen / Esc](#)[Printer-friendly Version](#)[Interactive Discussion](#)

In Fig. 5 the HOCl distribution of December 2003 is compared to that of July 2002. Particular low values (occasionally below 80 ppt at the maximum) are found in early winter higher midlatitudes, and seem to coincide with the polar vortex boundary region. The December 2003 monthly mean is dominated by measurements when the Northern polar vortex was still intact throughout all stratospheric altitudes, although a major warming happened in early January 2004, starting with a break-up of the vortex in the upper stratosphere in late December (Manney et al., 2005). During July 2002, the Antarctic vortex was still intact, although already the early winter was too warm (Krüger et al., 2005) and wave activity was observed (Newman and Nash, 2005), which later led to the unprecedented split of the Antarctic vortex. This feature, however, is observed in all winters and seems to have nothing to do with the particularly weak vortices of the examples shown.

Standard deviations are normally in the range of 50 to 80 ppt in the altitude of the mixing ratio maximum. Comparison to the estimated single profile error (appr. 40 ppt) suggests that the variability within a month and latitude bin is about 30 to 70 ppt. Under polar night conditions standard deviations often reach 150 ppt, reflecting displaced or inhomogeneously composed polar vortices.

A separated maximum is seen regularly in the lower polar winter stratosphere around 50–10 hPa. This feature has first been observed by von Clarmann et al. (2009a) in the Antarctic winter of 2002 but is now seen to appear regularly in Southern polar winters and occasionally also in northern polar winters, however to a lesser extent (Fig. 6). This maximum has been attributed to heterogeneous chemistry, presumably to heterogeneous ClO formation preceding gas-phase HOCl formation. The fact that this feature is more pronounced in southern polar winters is quite plausible and supports the hypothesis of being linked to heterogeneous chemistry, because it is well known that chlorine activation through heterogeneous chemistry is much more frequent and efficient in southern polar vortices. Austral winter chlorine activation from May until September 2002 onward has been reported by Feng et al. (2005). Very early chlorine activation was reported for the northern winter 2002/2003 by Tilmes et al. (2003), both

in consistence with our HOCl observations.

Figure 7 shows the temporal development of polar HOCl mixing ratios. Both the upper (3 hPa) and lower (20 hPa) polar winter maxima are clearly seen, as well as the illumination-dependent varying altitude of the maximum from local spring to fall.

The general shape of the distributions including the altitude of the maximal mixing ratio, the position of the summertime midlatitudinal maximum, the diurnal shift of the maximum, and the existence of a polar winter maximum are well reproduced by the model. However, modelled HOCl mixing ratios in the peak region around 10 hPa are lower by about 40 %. This discrepancy could be reconciled by the stronger temperature dependence of the $\text{ClO} + \text{HO}_2 \rightarrow \text{HOCl} + \text{O}_2$ reaction as measured by Stimpfle et al. (1979), compared to the JPL-06 rate constant recommendation (Sander et al., 2006) that is applied here. In contrast, the model largely overestimates HOCl during polar night.

The complete set of plots is available as Supplement from July 2002 to March 2004, and the data files in netcdf format will be made available via SPARC.

5.1 Particular events

During the observation period there were two very special events, which are scientifically interesting but require a caveat with respect to the climatological representativeness of the MIPAS data set. These are the split of the Antarctic polar vortex in the Austral winter of 2002, and the solar proton event around Halloween in 2003.

5.1.1 The split vortex event in 2002

The split vortex event in 2002 was characterized by a major warming (Allen et al., 2003; Sinnhuber et al., 2003; Krüger et al., 2005; Charlton et al., 2005) going along with pronounced wave activity involving planetary waves of wavenumber 1 to 3 (Wang et al., 2005) which led to a displacement, distortion, and finally a split of the polar vortex. While the lower stratospheric maximum of HOCl has been attributed to heterogeneous

The MIPAS HOCl climatology

T. von Clarmann et al.

Title Page

Abstract

Introduction

Conclusions

References

Tables

Figures

◀

▶

◀

▶

Back

Close

Full Screen / Esc

Printer-friendly Version

Interactive Discussion



chemistry, large HOCl amounts near 4 hPa have been attributed to exposure of Cl_y-rich polar vortex air to sunlight due to vortex displacement, triggering HO_x chemistry (von Clarmann et al., 2009a). Indeed, such large HOCl amounts were not observed in the Antarctic winter of 2003 (Fig. 8). The southern polar winter 2002 HOCl distributions resemble rather those of the northern winters within the observation period, where high HOCl concentrations at around 2 hPa seem to be the rule rather than the exception. This behaviour is not unexpected since due to larger northern hemispheric wave activity the polar vortex there is often displaced, distorted, and thus exposed to sunlight.

5.1.2 The Halloween solar storm in 2003

The Halloween solar proton event (SPE) in 2003 was one of the largest in the past forty years (Degenstein et al., 2005) and resulted in ozone depletion subsequent to HO_x, NO_x, NO_y and chlorine chemistry perturbations (Jackman et al., 2005; López-Puertas et al., 2005a,b; Jackman et al., 2008; Verronen et al., 2008). Observations of HOCl enhancements in response to the solar proton event gave evidence of perturbed chlorine chemistry as well as the first experimental evidence of perturbed HO_x chemistry (von Clarmann et al., 2005). These HO_x perturbations were later confirmed by direct hydroxyl observations (Verronen et al., 2006). Within the context of this climatological analysis it is important to note that HOCl measurements in October and November 2003 might not be representative for this season, although the observed HOCl enhancements were very localized and lasted only a few days and thus are not resolved in the monthly zonal means.

The MIPAS HOCl climatology

T. von Clarmann et al.

[Title Page](#)[Abstract](#)[Introduction](#)[Conclusions](#)[References](#)[Tables](#)[Figures](#)[◀](#)[▶](#)[◀](#)[▶](#)[Back](#)[Close](#)[Full Screen / Esc](#)[Printer-friendly Version](#)[Interactive Discussion](#)

6 Conclusions

The first global measurements covering nearly two annual cycles of stratospheric HOCl are presented. The most important features are (a) a mixing ratio maximum in summer midlatitudes at about 5 hPa; (b) an increase of the altitude of maximum mixing ratios during nighttime; (c) a minimum in winter high midlatitudes; (d) occasional enhancements in polar vortices, both in the altitude regimes of gas-phase and of heterogeneous chemistry. The observed features are generally well reproduced by the model calculations. Modelled mixing ratios, which are about 40 % lower than the observed ones, suggest that a reassessment of the $\text{HO}_2 + \text{ClO} \rightarrow \text{HOCl} + \text{O}_2$ reaction rate constant may be necessary, because the observations seem to be in better agreement with the kinetic data reported by Stimpfle et al. (1979). Large discrepancies between measurements and model in the mid-stratosphere during polar night require further attention.

The question to which extent this dataset is representative in a climatological sense or if it is dominated by particular atmospheric situations of the measurement period will be answered by a multi-instrument climatology involving also MLS and JEM/SMILES HOCl measurements.

Appendix A

Interpolation of standard deviation and number of measurements

Let $x_1 \dots x_m$ be the measurements in latitude bin 1, and $y_1 \dots y_n$ the measurements in latitude bin 2. Zonal means \bar{x} and \bar{y} in each of these bins are

$$\bar{x} = \frac{\sum_{i=1}^m x_i}{m} \tag{A1}$$

The MIPAS HOCl climatology

T. von Clarmann et al.

Title Page

Abstract

Introduction

Conclusions

References

Tables

Figures

◀

▶

◀

▶

Back

Close

Full Screen / Esc

Printer-friendly Version

Interactive Discussion



$$\bar{y} = \frac{\sum_{j=1}^n y_j}{n}.$$

Weighting by the inverse estimated error variances of the single measurements is intentionally not performed as to avoid biases due to atmospheric state dependent precision. For example, the MIPAS retrieval error is generally larger in a colder atmosphere, thus measurements in warmer parts of the atmosphere would be overrepresented. The standard deviation of the samples are

$$\sigma_x = \sqrt{\frac{\sum_{i=1}^m (x_i - \bar{x})^2}{m - 1}} \quad (\text{A2})$$

$$\sigma_y = \sqrt{\frac{\sum_{j=1}^n (y_j - \bar{y})^2}{n - 1}}.$$

The interpolation to the desired latitude is

$$\bar{z} = (v, w) \begin{pmatrix} \bar{x} \\ \bar{y} \end{pmatrix} = v \bar{x} + w \bar{y} \quad (\text{A3})$$

where v and w are weighting factors depending on the distances between the initial mean measurement geolocations l_x and l_y and the geolocation of the interpolated measurement l_z :

$$v = \frac{l_z - l_y}{l_x - l_y} = 1 - \frac{l_x - l_z}{l_x - l_y} \quad (\text{A4})$$

$$w = 1 - v$$

The MIPAS HOCl climatology

T. von Clarmann et al.

Title Page	
Abstract	Introduction
Conclusions	References
Tables	Figures
◀	▶
◀	▶
Back	Close
Full Screen / Esc	
Printer-friendly Version	
Interactive Discussion	



The standard deviation σ_z of the interpolated mixing ratio is, according to generalized Gaussian error estimation

$$\begin{aligned}\sigma_z &= \sqrt{(v, w) \begin{pmatrix} \sigma_x^2 & r \sigma_x \sigma_y \\ r \sigma_x \sigma_y & \sigma_y^2 \end{pmatrix} \begin{pmatrix} v \\ w \end{pmatrix}} \\ &= \sqrt{v^2 \sigma_x^2 + 2 v w r \sigma_x \sigma_y + w^2 \sigma_y^2}.\end{aligned}\quad (\text{A5})$$

For fully correlated x and y this reduces to simple linear interpolation of the standard deviation while for fully independent x and y this reduces to quadratic interpolation of variances. It is important to note, that interpolation of covariance matrices from a coarser to a finer grid does not represent fine-scale variability which does not show up in the coarse grid. This caveat, however, does not apply to the application of this paper, because the target latitude grid is coarser than the initial one on which the MIPAS measurements were performed.

The virtual number of measurements

The data format of the SPARC Data Initiative also requires the number of measurements k used to calculate the zonal mean. Also this quantity is not trivial to interpolate. We argue that the purpose of this quantity is that the user can calculate the standard error of the mean, σ_{stderr} . The usual recipe for this purpose assumes independent data and is

$$\sigma_{\text{stderr}} = \frac{\sigma}{\sqrt{k}}.\quad (\text{A6})$$

We argue that the most useful estimate of the number of observations is that where Eq. (A6) holds, regardless how the standard deviation σ was obtained. We thus define a “virtual number of measurements”, k_v , which is defined as

$$k_v = \sigma^2 / \sigma_{\text{stderr}}^2\quad (\text{A7})$$

The direct estimate of the interpolated zonal mean z from the single measurements x_j and y_j is (averaging and interpolation in one step)

$$z = \left(\frac{v_1}{m} \dots \frac{v_m}{m}; \frac{w_1}{n} \dots \frac{w_n}{n} \right) \begin{pmatrix} x_1 \\ \vdots \\ x_m \\ y_1 \\ \vdots \\ y_m \end{pmatrix} = \mathbf{g}^T \begin{pmatrix} x_1 \\ \vdots \\ x_m \\ y_1 \\ \vdots \\ y_m \end{pmatrix} \quad (\text{A8})$$

The standard error of z is calculated by generalized Gaussian error propagation. We assume $m \leq n$ to allow for additional measurements in one bin without counterpart in the other bin). We further assume zero correlation between multiple measurements within one latitude bin; this approximation is justified because these measurements belong mostly to different orbits, and with MIPAS it takes about three days until the same geolocation is observed again. In contrast, correlations between subsequent measurements of the same orbit but different latitude bins are considered, because these measurements are only 70 s and 510 km apart.

$$\sigma_{z,\text{stderr}}^2 = \mathbf{g}^T \begin{pmatrix} \sigma_x^2 & & 0 & r \sigma_x \sigma_y & & 0 & 0 & \dots & 0 \\ & \ddots & & & & & & \ddots & \vdots \\ 0 & & \sigma_x^2 & 0 & & r \sigma_x \sigma_y & 0 & \dots & 0 \\ r \sigma_x \sigma_y & & 0 & \sigma_y^2 & & 0 & 0 & \dots & 0 \\ & \ddots & & & \ddots & & & \ddots & \vdots \\ 0 & & r \sigma_x \sigma_y & 0 & & \sigma_y^2 & 0 & \dots & 0 \\ 0 & \dots & 0 & 0 & \dots & 0 & \sigma_y^2 & & 0 \\ \vdots & & & & \vdots & & & \ddots & \\ 0 & \dots & 0 & 0 & \dots & 0 & 0 & & \sigma_y^2 \end{pmatrix} \mathbf{g} \quad (\text{A9})$$

$$= \sum_{i=1}^m \frac{v_i^2 \sigma_x^2}{m^2} + \sum_{j=1}^n \frac{w_j^2 \sigma_y^2}{n^2} + 2 \sum_{i=1}^m \frac{rvw \sigma_x \sigma_y}{m}$$

The MIPAS HOCl climatology

T. von Clarmann et al.

Title Page	
Abstract	Introduction
Conclusions	References
Tables	Figures
◀	▶
◀	▶
Back	Close
Full Screen / Esc	
Printer-friendly Version	
Interactive Discussion	



With σ_z obtained from Eq. (A5) and $\sigma_{z,\text{stderr}}^2$ obtained from Eq. (A9), the virtual number of measurements k_v can be calculated using Eq. (A7). Although the result can be a fraction, in order not to confuse the user and to comply with the data format of the SPARC Data Initiative, we round the result to the nearest lower integer.

Estimation of the correlation coefficient

Ideally the correlation coefficient r can be calculated in a straight forward manner along with the zonal means and their standard deviations. However, the given data structure may be obstructive for this purpose. We thus propose a scheme to estimate r without going back to the single measurements. We assume that the total observed variability σ_{observed} (e.g. σ_x or σ_y) is composed of measurement error σ_{noise} and natural variability σ_{nat} as

$$\sigma_{\text{observed}}^2 = \sigma_{\text{noise}}^2 + \sigma_{\text{nat}}^2 \quad (\text{A10})$$

Measurement errors are in good approximation uncorrelated between subsequent measurements ($r_{\text{noise}} = 0$) while natural variations are supposed to be highly correlated ($r_{\text{nat}} \approx 1$) between subsequent measurements. We infer r by decomposing each value in a true component ($x_{i,\text{true}}$ and $y_{i,\text{true}}$, respectively) and a noise term (ϵ_i and γ_i , respectively):

$$r = \frac{\sum_{i=1}^m (x_i - \bar{x}) (y_i - \bar{y})}{(m-1) \sigma_x \sigma_y} = \frac{\sum_{i=1}^m (x_{i,\text{true}} - \bar{x}) (y_{i,\text{true}} - \bar{y})}{(m-1) \sigma_x \sigma_y} \quad (\text{A11})$$

$$+ \frac{\sum_{i=1}^m (x_{i,\text{true}} - \bar{x}) \gamma_i}{(m-1) \sigma_x \sigma_y} + \frac{\sum_{i=1}^m (y_{i,\text{true}} - \bar{y}) \epsilon_i}{(m-1) \sigma_x \sigma_y} + \frac{\sum_{i=1}^m \epsilon_i \gamma_i}{(m-1) \sigma_x \sigma_y},$$

Title Page

Abstract

Introduction

Conclusions

References

Tables

Figures

◀

▶

◀

▶

Back

Close

Full Screen / Esc

Printer-friendly Version

Interactive Discussion



where the latter three terms are ignored because the noise terms are assumed to be uncorrelated and thus to have a tendency to cancel out. With

$$a = \frac{\sigma_{x,\text{nat}}}{\sigma_x} \quad (\text{A12})$$

and

$$b = \frac{\sigma_{y,\text{nat}}}{\sigma_y} \quad (\text{A13})$$

we can rewrite the surviving term of Eq. (A11) as

$$r = ab \frac{\sum_{i=1}^m (x_{i,\text{true}} - \bar{x}) (y_{i,\text{true}} - \bar{y})}{(m-1) \sigma_x \sigma_y} \quad (\text{A14})$$
$$= ab \frac{\sqrt{\sigma_x^2 - \sigma_{x,\text{noise}}^2} \sqrt{\sigma_y^2 - \sigma_{y,\text{noise}}^2}}{\sigma_x \sigma_y}$$

Since both the observed standard deviations σ_x and σ_y and error estimates $\sigma_{x,\text{noise}}$ and $\sigma_{y,\text{noise}}$ are available for MIPAS retrievals, we can estimate r without retrieving information which pairs of measurements x_i and y_i belong together.

Supplementary material related to this article is available online at:

**[http://www.atmos-chem-phys-discuss.net/11/20793/2011/
acpd-11-20793-2011-supplement.zip](http://www.atmos-chem-phys-discuss.net/11/20793/2011/acpd-11-20793-2011-supplement.zip)**

Acknowledgements. The retrievals of IMK/IAA were performed on the HP XC4000 of the Scientific Supercomputing Center (SSC) Karlsruhe under project grant MIPAS. IMK data analysis was supported by DLR under contract number 50EE0901. BF was supported by the Spanish project AYA200803498/ESP by the project 200950I081 of CSIC. MIPAS level 1B data were provided by ESA.

References

- Abbatt, J. P. D. and Molina, M. J.: The Heterogeneous Reaction $\text{HOCl} + \text{HCl} \rightarrow \text{Cl}_2 + \text{H}_2\text{O}$ on ice and nitric acid trihydrate: Reaction probabilities and stratospheric implications, *Geophys. Res. Lett.*, 19, 461–464, doi:10.1029/92GL00373, 1992. 20794
- 5 Allen, D. R., Bevilacqua, R. M., Nedoluha, G. E., Randall, C. E., and Manney, G. L.: Unusual stratospheric transport and mixing during the 2002 Antarctic winter, *Geophys. Res. Lett.*, 30, 1599, doi:10.1029/2003GL017117, 2003. 20801
- Chance, K., Traub, W. A., Johnson, D. G., Jucks, K. W., Ciarpallini, P., Stachnik, R. A., Salawitch, R. J., and Michelsen, H. A.: Simultaneous measurements of stratospheric HO_x , NO_x and Cl_x ; Comparison with a photochemical model, *J. Geophys. Res.*, 101, 9031–9043, 1996. 20797, 20799
- 10 Chance, K. V., Johnson, D. G., and Traub, W. A.: Measurement of stratospheric HOCl: Concentration profiles, including diurnal variation, *J. Geophys. Res.*, 94, 11059–11069, 1989. 20795, 20797, 20799
- 15 Charlton, A. J., O'Neill, A., Lahoz, W. A., and Berrisford, P.: The splitting of the stratospheric polar vortex in the southern hemisphere, September 2002: Dynamical evolution, *J. Atmos. Sci.*, 62, 590–602, 2005. 20801
- Chauhan, S., Höpfner, M., Stiller, G. P., von Clarmann, T., Funke, B., Glatthor, N., Grabowski, U., Linden, A., Kellmann, S., Milz, M., Steck, T., Fischer, H., Froidevaux, L., Lambert, A., Santee, M. L., Schwartz, M., Read, W. G., and Livesey, N. J.: MIPAS reduced spectral resolution UTLS-1 mode measurements of temperature, O_3 , HNO_3 , N_2O , H_2O and relative humidity over ice: retrievals and comparison to MLS, *Atmos. Meas. Tech.*, 2, 337–353, doi:10.5194/amt-2-337-2009, 2009. 20796
- 20 Cofield, R. E. and Stek, P. C.: Design and field-of-view calibration of 114–660 GHz optics of the Earth Observing System Microwave Limb Sounder, *IEEE T. Geosci. Remote*, 44, 1166–1181, 2006. 20795
- 25 Crutzen, P. J., Müller, R., Brühl, C., and Peter, T.: On The Potential Importance of the Gase Phase Reaction $\text{CH}_3\text{O}_2 + \text{ClO} \rightarrow \text{ClOO} + \text{CH}_3\text{O}$ and the Heterogeneous Reaction $\text{HOCl} + \text{HCl} \rightarrow \text{H}_2\text{O} + \text{Cl}_2$ in “Ozone Hole” Chemistry, *Geophys. Res. Lett.*, 19, 1113–1116, 1992. 20794
- 30

Title Page

Abstract

Introduction

Conclusions

References

Tables

Figures

◀

▶

◀

▶

Back

Close

Full Screen / Esc

Printer-friendly Version

Interactive Discussion



**The MIPAS HOCl
climatology**

T. von Clarmann et al.

[Title Page](#)[Abstract](#)[Introduction](#)[Conclusions](#)[References](#)[Tables](#)[Figures](#)[◀](#)[▶](#)[◀](#)[▶](#)[Back](#)[Close](#)[Full Screen / Esc](#)[Printer-friendly Version](#)[Interactive Discussion](#)

- Degenstein, D. A., Lloyd, N. D., Bourassa, A. E., Gattinger, R. L., and Llewellyn, E. J.: Observations of mesospheric ozone depletion during the October 28, 2003 solar proton event by OSIRIS, *Geophys. Res. Lett.*, 32, L03S11, doi:10.1029/2004GL021521, 2005. 20802
- Feng, W., Chipperfield, M. P., Roscoe, H. K., Remedios, J. J., Waterfall, A. M., Stiller, G. P., Glatthor, N., Höpfner, M., and Wang, D.-Y.: Three-dimensional Model Study of the Antarctic Ozone Hole in 2002 and Comparison with 2000, *J. Atmos. Sci.*, 62, 822–837, 2005. 20800
- Fischer, H., Birk, M., Blom, C., Carli, B., Carlotti, M., von Clarmann, T., Delbouille, L., Dudhia, A., Ehhalt, D., Endemann, M., Flaud, J. M., Gessner, R., Kleinert, A., Koopman, R., Langen, J., López-Puertas, M., Mosner, P., Nett, H., Oelhaf, H., Perron, G., Remedios, J., Ridolfi, M., Stiller, G., and Zander, R.: MIPAS: an instrument for atmospheric and climate research, *Atmos. Chem. Phys.*, 8, 2151–2188, doi:10.5194/acp-8-2151-2008, 2008. 20795
- Hanson, D. R. and Ravishankara, A. R.: Investigation of the reactive and nonreactive processes involving ClONO₂ and HCl on water and nitric acid doped ice, *J. Phys. Chem.*, 96, 2682–2691, 1992. 20794
- Hegglin, M. and Tegtmeier, S.: The SPARC Data Initiative, *SPARC Newsletter*, 36, 22–23, 2011. 20797
- IPCC: A contribution of Working Groups I, II and III to the Third Assessment Report of the Intergovernmental Panel on Climate Change, in: *Climate Change 2001: Synthesis Report*, edited by: Watson, R. T. and the Core Writing Team, Cambridge University Press, Cambridge, UK, and New York, USA, 2001. 20798
- Jackman, C. H., DeLand, M. T., Labow, G. J., Fleming, E. L., Weisenstein, D. K., Ko, M. K. W., Sinnhuber, M., and Russell, J. M.: Neutral atmospheric influences of the solar proton events in October–November 2003, *J. Geophys. Res.*, 110, A09S27, doi:10.1029/2004JA010888, 2005. 20802
- Jackman, C. H., Marsh, D. R., Vitt, F. M., Garcia, R. R., Fleming, E. L., Labow, G. J., Randall, C. E., López-Puertas, M., Funke, B., von Clarmann, T., and Stiller, G. P.: Short- and medium-term atmospheric constituent effects of very large solar proton events, *Atmos. Chem. Phys.*, 8, 765–785, doi:10.5194/acp-8-765-2008, 2008. 20796, 20802
- Jöckel, P., Sander, R., Kerkweg, A., Tost, H., and Lelieveld, J.: Technical Note: The Modular Earth Submodel System (MESSy) – a new approach towards Earth System Modeling, *Atmos. Chem. Phys.*, 5, 433–444, doi:10.5194/acp-5-433-2005, 2005. 20798

The MIPAS HOCl climatology

T. von Clarmann et al.

Title Page

Abstract

Introduction

Conclusions

References

Tables

Figures

◀

▶

◀

▶

Back

Close

Full Screen / Esc

Printer-friendly Version

Interactive Discussion



- Jöckel, P., Tost, H., Pozzer, A., Brühl, C., Buchholz, J., Ganzeveld, L., Hoor, P., Kerkgeweg, A., Lawrence, M. G., Sander, R., Steil, B., Stiller, G., Tanarhte, M., Taraborrelli, D., van Aardenne, J., and Lelieveld, J.: The atmospheric chemistry general circulation model ECHAM5/MESSy1: consistent simulation of ozone from the surface to the mesosphere, *Atmos. Chem. Phys.*, 6, 5067–5104, doi:10.5194/acp-6-5067-2006, 2006. 20798
- Johnson, D. G., Traub, W. A., Chance, K. V., Jucks, K. W., and Stachnik, R. A.: Estimating the abundance of ClO from simultaneous remote sensing measurements of HO₂, OH, and HOCl, *Geophys. Res. Lett.*, 22, 1869–1871, 1995. 20795
- Kasai, Y. J., Baron, P., Ochiai, S., Mendrok, J., Urban, J., Murtagh, D., Moller, J., Manabe, T., Kikuchi, K., and Nishibori, T.: JEM/SMILES observation capability, in: *Sensors, Systems, and Next-Generation Satellites XIII*, edited by: Meynart, R., Neeck, S. P., and Shimoda, H., SPIE, 7474, 74740S, doi:10.1117/12.830825, 2009. 20795
- Kirner, O.: *Prozessstudien der stratosphärischen Chemie und Dynamik mit Hilfe des Chemie-Klima-Modells ECHAM5/MESSy1*, Ph.D. thesis, Universität Karlsruhe, Germany, 2008. 20799
- Kirner, O., Ruhnke, R., Buchholz-Dietsch, J., Jöckel, P., Brühl, C., and Steil, B.: Simulation of polar stratospheric clouds in the chemistry-climate-model EMAC via the submodel PSC, *Geosci. Model Dev.*, 4, 169–182, doi:10.5194/gmd-4-169-2011, 2011. 20799
- Kovalenko, L. J., Jucks, K. W., Salawitch, R. J., Toon, G. C., Blavier, J.-F., Johnson, D. G., Kleinböhl, A., Livesey, N. J., Margitan, J. J., Pickett, H. M., Santee, M. L., Sen, B., Stachnik, R. A., and Waters, J. W.: Observed and modeled HOCl profiles in the midlatitude stratosphere: Implication for ozone loss, *Geophys. Res. Lett.*, 34, L19801, doi:10.1029/2007GL031100, 2007. 20795
- Krüger, K., Naujokat, B., and Labitzke, K.: The Unusual Midwinter Warming in the Southern Hemisphere Stratosphere 2002: A Comparison to Northern Hemisphere Phenomena, *J. Atmos. Sci.*, 62, 603–613, 2005. 20800, 20801
- Larsen, J. C., Rinsland, C. P., Goldman, A., Murcray, D. G., and Murcray, F. J.: Upper Limits for Stratospheric H₂O₂ and HOCl from High Resolution Balloon-Borne Infrared Solar Absorption Spectra, *Geophys. Res. Lett.*, 12, 663–666, 1985. 20795
- López-Puertas, M., Funke, B., Gil-López, S., von Clarmann, T., Stiller, G. P., Höpfner, M., Kellmann, S., Fischer, H., and Jackman, C. H.: Observation of NO_x Enhancement and Ozone Depletion in the Northern and Southern Hemispheres after the October–November 2003 Solar Proton Events, *J. Geophys. Res.*, 110, A09S43, doi:10.1029/2005JA011050, 2005a.

20802

López-Puertas, M., Funke, B., Gil-López, S., von Clarmann, T., Stiller, G. P., Höpfner, M., Kellmann, S., Mengistu Tsidu, G., Fischer, H., and Jackman, C. H.: HNO₃, N₂O₅ and ClONO₂ Enhancements after the October–November 2003 Solar Proton Events, *J. Geophys. Res.*, 110, A09S44, doi:10.1029/2005JA011051, 2005b. 20802

Manney, G. L., Krüger, K., Sabutis, J. L., Sena, S. A., and Pawson, S.: The remarkable 2003–2004 winter and other recent warm winters in the Arctic stratosphere since the late 1990s, *J. Geophys. Res.*, 110, D04107, doi:10.1029/2004JD005367, 2005. 20800

Newman, P. A. and Nash, E. R.: The Unusual Southern Hemisphere Stratosphere Winter of 2002, *J. Atmos. Sci.*, 62, 614–628, 2005. 20800

Prather, M. J.: More rapid polar ozone depletion through the reaction of HOCl with HCl on polar stratospheric clouds, *Nature*, 355, 534–537, 1992. 20794

Prinn, R. G., Huang, J., Weiss, R. F., Cunnold, D. M., Fraser, P. J., Simmonds, P. G., McCulloch, A., Harth, C., Salameh, P., Doherty, S., Wang, R. H. J., Porter, L., and Miller, B. R.: Evidence for substantial variations of atmospheric hydroxyl radicals in the past two decades, *Science*, 292, 1882–1888, 2001. 20798

Raper, O. F., Farmer, C. B., Zander, R., and Park, J. H.: Infrared Spectroscopic Measurements of Halogenated Sink and Reservoir Gases in the Stratosphere With the ATMOS Instrument, *J. Geophys. Res.*, 92, 9851–9858, 1987. 20795

Roeckner, E., Brokopf, R., Esch, M., Giorgetta, M., Hagemann, S., Koernblueh, L., Manzini, E., Schlese, U., and Schulzweida, U.: Sensitivity of simulated climate to horizontal and vertical resolution in the ECHAM5 atmosphere model, *J. Climate*, 19, 3771–3791, 2006. 20798

Sander, R., Kerkweg, A., Jöckel, P., and Lelieveld, J.: Technical note: The new comprehensive atmospheric chemistry module MECCA, *Atmos. Chem. Phys.*, 5, 445–450, doi:10.5194/acp-5-445-2005, 2005. 20798

Sander, S. P., Golden, D. M., Kurylo, M. J., Moortgat, G. K., Wine, P. H., Ravishankara, A. R., Kolb, C. E., Molina, M. J., Finlayson-Pitts, B. J., Huie, R. E., Orkin, V. L., Friedl, R. R., and Keller-Rudek, H.: Chemical kinetics and photochemical data for use in atmospheric studies: evaluation number 15, JPL Publication 06-2, Jet Propulsion Laboratory, California Institute of Technology, Pasadena, CA, 2006. 20795, 20801

Sinnhuber, B.-M., Weber, M., Amankwah, A., and Burrows, J. P.: Total ozone during the unusual Antarctic winter of 2002, *Geophys. Res. Lett.*, 30, 1580, doi:10.1029/2002GL016798, 2003. 20801

20812

ACPD

11, 20793–20822, 2011

The MIPAS HOCl climatology

T. von Clarmann et al.

Title Page

Abstract

Introduction

Conclusions

References

Tables

Figures

◀

▶

◀

▶

Back

Close

Full Screen / Esc

Printer-friendly Version

Interactive Discussion



- Solomon, S., Garcia, R. R., Rowland, F. S., and Wuebbles, D. J.: On the depletion of Antarctic ozone, *Nature*, 321, 755–758, 1986. 20794
- Steck, T. and von Clarmann, T.: Constrained profile retrieval applied to the observation mode of the Michelson Interferometer for Passive Atmospheric Sounding, *Appl. Optics*, 40, 3559–3571, 2001. 20796
- 5 Stimpfle, R. M., Perry, R. A., and Howard, C. J.: Temperature-dependence of the reaction of ClO and HO₂ radicals, *J. Chem. Phys.*, 71, 5183–5190, 1979. 20795, 20801, 20803
- Tilmes, S., Müller, R., Groöß, J.-U., Höpfner, M., Toon, G. C., and Russell III, J. M.: Very early chlorine activation and ozone loss in the Arctic winter 2002–2003, *Geophys. Res. Lett.*, 30, 2201, doi:10.1029/2003GL018079, 2003. 20800
- 10 Toon, G. C., Farmer, C. B., Schaper, P. W., Lowes, L. L., and Norton, R. H.: Composition measurements of the 1989 Arctic winter stratosphere by airborne infrared solar absorption spectroscopy, *J. Geophys. Res.*, 97, 7939–7961, 1992. 20795
- Traub, W. A., Johnson, D. G., and Chance, K. V.: Stratospheric Hydroperoxyl Measurements, *Science*, 247, 446–449, 1990. 20795
- 15 Verronen, P. T., Seppälä, A., Kyrölä, E., Tamminen, J., Pickett, H. M., and Turunen, E.: Production of odd hydrogen in the mesosphere during the January 2005 solar proton event, *Geophys. Res. Lett.*, 33, L24811, doi:10.1029/2006GL028115, 2006. 20802
- Verronen, P. T., Funke, B., López-Puertas, M., Stiller, G. P., von Clarmann, T., Glatthor, N., Enell, C.-F., Turunen, E., and Tamminen, J.: About the increase of HNO₃ in the stratopause region during the Halloween 2003 solar proton event, *Geophys. Res. Lett.*, 35, L20809, doi:10.1029/2008GL035312, 2008. 20802
- 20 von Clarmann, T., Wetzels, G., Oelhaf, H., Friedl-Vallon, F., Linden, A., Maucher, G., Seefeldner, M., Trieschmann, O., and Lefèvre, F.: ClONO₂ vertical profile and estimated mixing ratios of ClO and HOCl in winter Arctic stratosphere from Michelson Interferometer for Passive Atmospheric Sounding limb emission spectra, *J. Geophys. Res.*, 102, 16157–16168, 1997. 20795
- 25 von Clarmann, T., Glatthor, N., Grabowski, U., Höpfner, M., Kellmann, S., Kiefer, M., Linden, A., Mengistu Tsidu, G., Milz, M., Steck, T., Stiller, G. P., Wang, D. Y., Fischer, H., Funke, B., Gil-López, S., and López-Puertas, M.: Retrieval of temperature and tangent altitude pointing from limb emission spectra recorded from space by the Michelson Interferometer for Passive Atmospheric Sounding (MIPAS), *J. Geophys. Res.*, 108, 4736, doi:10.1029/2003JD003602, 2003. 20796
- 30

**The MIPAS HOCl
climatology**

T. von Clarmann et al.

Title Page

Abstract

Introduction

Conclusions

References

Tables

Figures

◀

▶

◀

▶

Back

Close

Full Screen / Esc

Printer-friendly Version

Interactive Discussion



**The MIPAS HOCl
climatology**

T. von Clarmann et al.

[Title Page](#)[Abstract](#)[Introduction](#)[Conclusions](#)[References](#)[Tables](#)[Figures](#)[◀](#)[▶](#)[◀](#)[▶](#)[Back](#)[Close](#)[Full Screen / Esc](#)[Printer-friendly Version](#)[Interactive Discussion](#)

- von Clarmann, T., Glatthor, N., Höpfner, M., Kellmann, S., Ruhnke, R., Stiller, G. P., Fischer, H., Funke, B., Gil-López, S., and López-Puertas, M.: Experimental Evidence of Perturbed Odd Hydrogen and Chlorine Chemistry After the October 2003 Solar Proton Events, *J. Geophys. Res.*, 110, A09S45, doi:10.1029/2005JA011053, 2005. 20794, 20802
- 5 von Clarmann, T., Glatthor, N., Grabowski, U., Höpfner, M., Kellmann, S., Linden, A., Mengistu Tsidu, G., Milz, M., Steck, T., Stiller, G. P., Fischer, H., and Funke, B.: Global stratospheric HOCl distributions retrieved from infrared limb emission spectra recorded by the Michelson Interferometer for Passive Atmospheric Sounding (MIPAS), *J. Geophys. Res.*, 111, D05311, doi:10.1029/2005JD005939, 2006. 20795, 20796, 20797
- 10 von Clarmann, T., Glatthor, N., Ruhnke, R., Stiller, G. P., Kirner, O., Reddmann, T., Höpfner, M., Kellmann, S., Kouker, W., Linden, A., and Funke, B.: HOCl chemistry in the Antarctic Stratospheric Vortex 2002, as observed with the Michelson Interferometer for Passive Atmospheric Sounding (MIPAS), *Atmos. Chem. Phys.*, 9, 1817–1829, doi:10.5194/acp-9-1817-2009, 2009a. 20794, 20795, 20800, 20802
- 15 von Clarmann, T., Höpfner, M., Kellmann, S., Linden, A., Chauhan, S., Funke, B., Grabowski, U., Glatthor, N., Kiefer, M., Schieferdecker, T., Stiller, G. P., and Versick, S.: Retrieval of temperature, H₂O, O₃, HNO₃, CH₄, N₂O, ClONO₂ and ClO from MIPAS reduced resolution nominal mode limb emission measurements, *Atmos. Meas. Tech.*, 2, 159–175, doi:10.5194/amt-2-159-2009, 2009b. 20796
- 20 Wang, D. Y., von Clarmann, T., Fischer, H., Funke, B., García-Comas, M., Gil-López, S., Glatthor, N., Grabowski, U., Höpfner, M., Kellmann, S., Kiefer, M., Koukouli, M. E., Lin, G., Linden, A., López-Puertas, M., Mengistu Tsidu, G., Milz, M., Steck, T., and Stiller, G. P.: Longitudinal variations of temperature and ozone profiles observed by MIPAS during the Antarctic stratosphere sudden warming of 2002, *J. Geophys. Res.*, 110, D20101, doi:10.1029/2004JD005749, 2005. 20801
- 25 World Meteorological Organization: Scientific Assessment of Ozone Depletion: 2006, Global Ozone Research and Monitoring Project – Report No. 50, Geneva, Switzerland, 572 pp., 2007. 20798

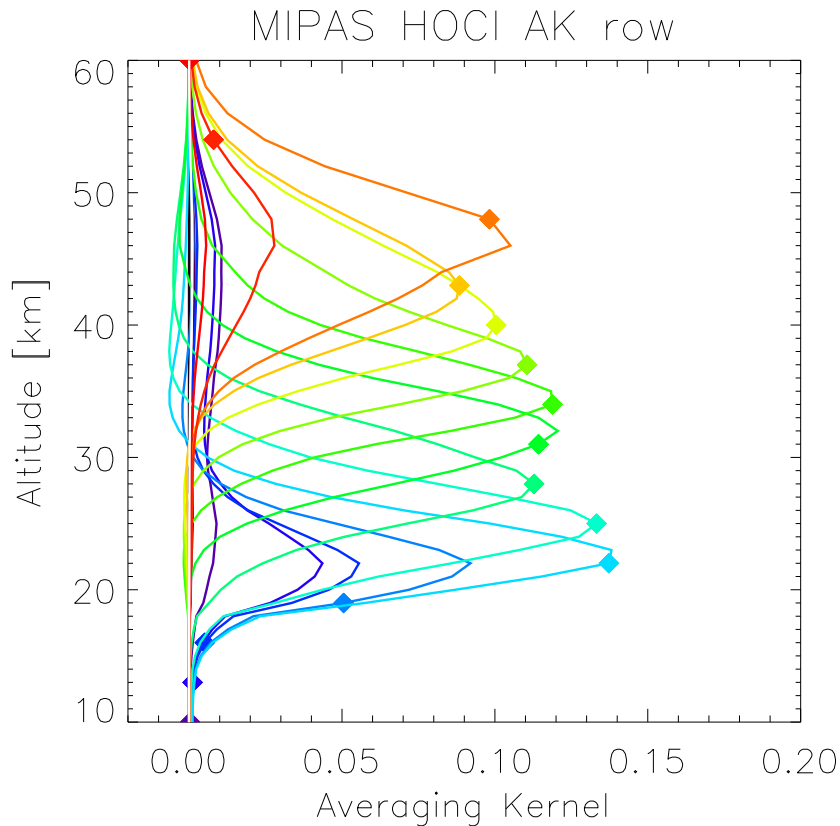


Fig. 1. Averaging kernels of MIPAS HOCl measurements. Diamonds represent the nominal altitudes (i.e. the diagonal value of the averaging kernel matrix). For clarity, only every third averaging kernel is shown. This example refers to a profile measured during night at 27.9° S, 86.2° E on 1 January 2003, 16:34 UT.

Title Page	
Abstract	Introduction
Conclusions	References
Tables	Figures
◀	▶
◀	▶
Back	Close
Full Screen / Esc	
Printer-friendly Version	
Interactive Discussion	



The MIPAS HOCl climatology

T. von Clarmann et al.

Title Page

Abstract

Introduction

Conclusions

References

Tables

Figures

◀

▶

◀

▶

Back

Close

Full Screen / Esc

Printer-friendly Version

Interactive Discussion

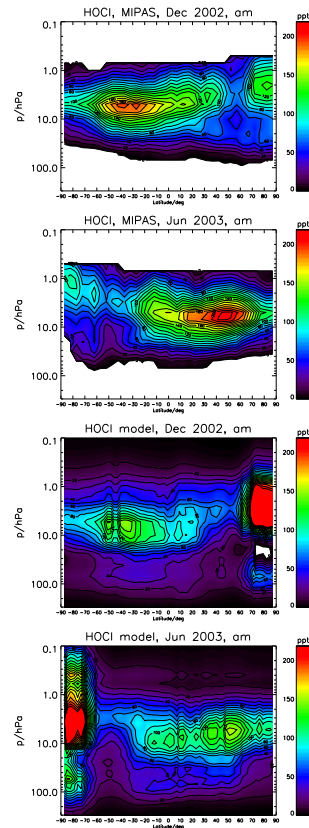


Fig. 2. Zonal mean HOCl distribution in December 2002 (top panel) and June 2003 (second panel). Measurements taken during the descending part of the orbit, i.e. morning measurements, are shown. The maximum mixing ratios are found at lower altitudes in the summer hemisphere. White areas represent altitudes where MIPAS was not sensitive to HOCl. The lower panels represent the respective model calculations, after application of MIPAS averaging kernels. White areas in the model fields represent negative data caused by side wiggles of MIPAS averaging kernels.

The MIPAS HOCl climatology

T. von Clarmann et al.

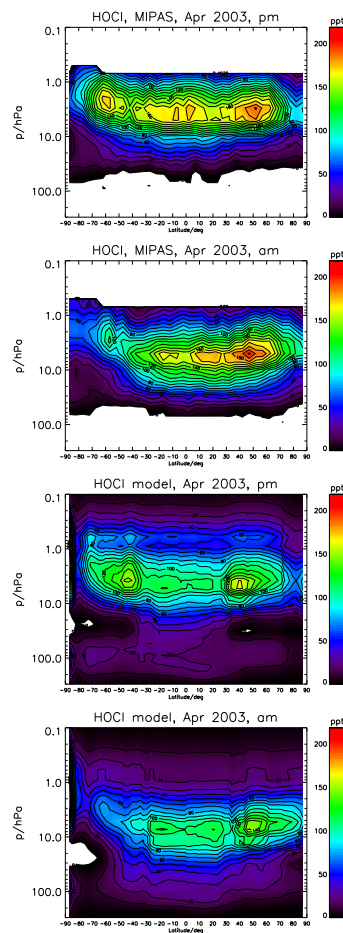


Fig. 3. MIPAS zonal mean HOCl distribution in April 2003 at 10:00 p.m. (top panel) and 10:00 a.m. (second panel), and related model calculations (third and fourth panel).

[Title Page](#)[Abstract](#)[Introduction](#)[Conclusions](#)[References](#)[Tables](#)[Figures](#)[◀](#)[▶](#)[◀](#)[▶](#)[Back](#)[Close](#)[Full Screen / Esc](#)[Printer-friendly Version](#)[Interactive Discussion](#)

The MIPAS HOCl climatology

T. von Clarmann et al.

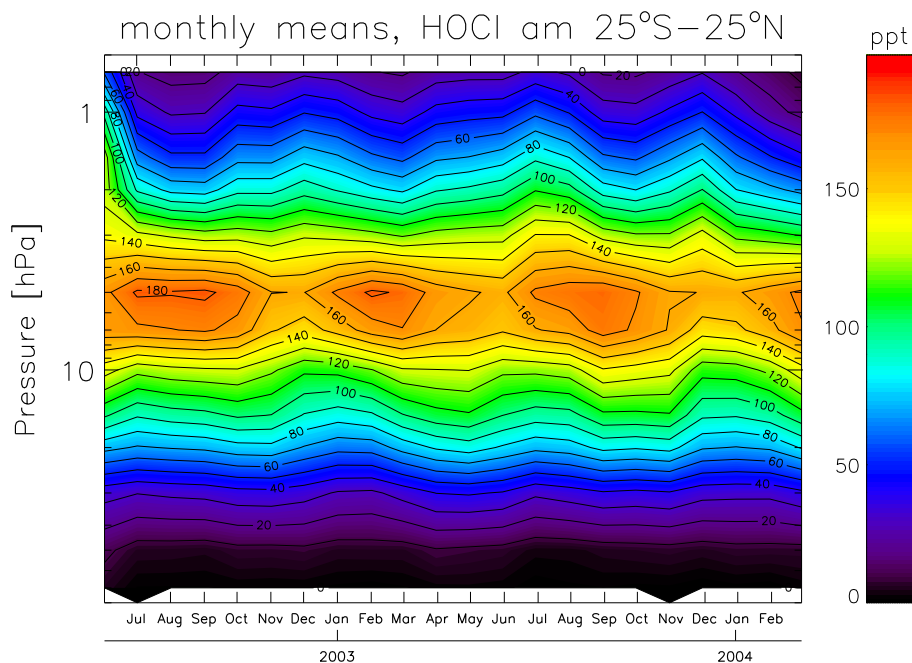


Fig. 4. Timeseries of HOCl zonal mean molar mixing ratios for the equatorial region 25° S–25° N. Measurements of the descending part of the orbit (10:00 a.m.) are shown.

[Title Page](#)[Abstract](#)[Introduction](#)[Conclusions](#)[References](#)[Tables](#)[Figures](#)[◀](#)[▶](#)[◀](#)[▶](#)[Back](#)[Close](#)[Full Screen / Esc](#)[Printer-friendly Version](#)[Interactive Discussion](#)

The MIPAS HOCl climatology

T. von Clarmann et al.

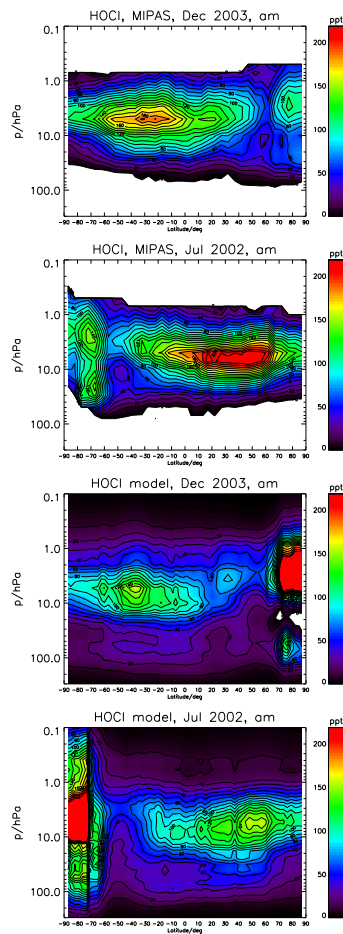


Fig. 5. Zonal mean morning HOCl distribution in Arctic (top panel) and Antarctic (second panel) winters (December 2003 and July 2002, respectively). Note low values in sub-polar regions. The third and fourth panel represent the respective model data sets.

[Title Page](#)[Abstract](#)[Introduction](#)[Conclusions](#)[References](#)[Tables](#)[Figures](#)[◀](#)[▶](#)[◀](#)[▶](#)[Back](#)[Close](#)[Full Screen / Esc](#)[Printer-friendly Version](#)[Interactive Discussion](#)

The MIPAS HOCl climatology

T. von Clarmann et al.

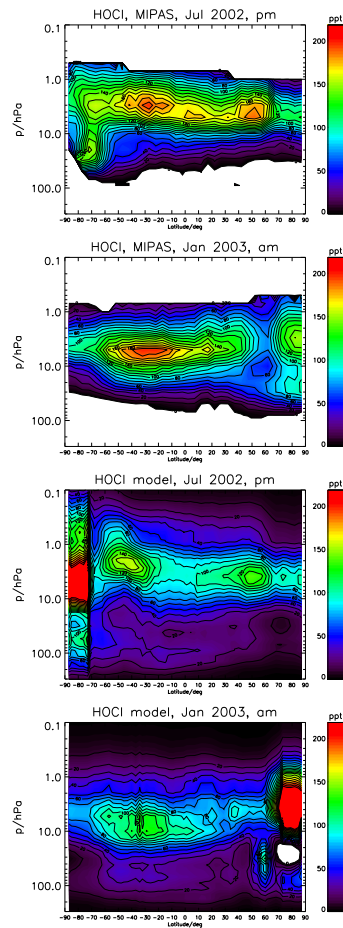


Fig. 6. Increased HOCl amounts in the southern (July 2002, evening, upper panel) and northern (January 2003, morning, second panel) polar winter stratospheric vortex subsequent to chlorine activation, together with related model calculations (third and fourth panel).

[Title Page](#)[Abstract](#)[Introduction](#)[Conclusions](#)[References](#)[Tables](#)[Figures](#)[◀](#)[▶](#)[◀](#)[▶](#)[Back](#)[Close](#)[Full Screen / Esc](#)[Printer-friendly Version](#)[Interactive Discussion](#)

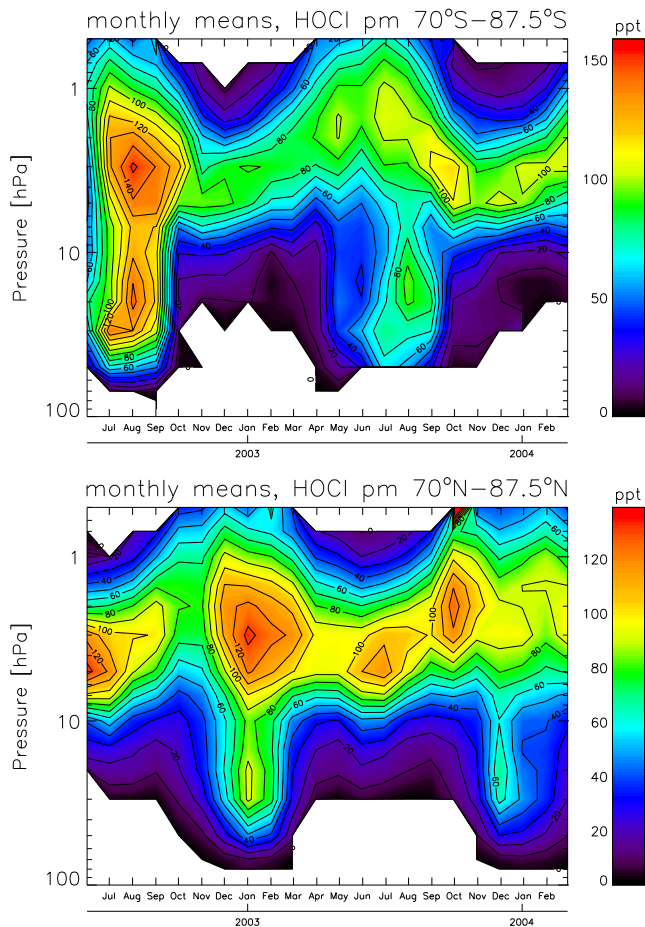


Fig. 7. Timeseries of HOCl zonal mean molar mixing ratios poleward of 70° for the Antarctic (upper panel) and the Arctic (lower panel). Measurements of the ascending part of the orbit are shown.

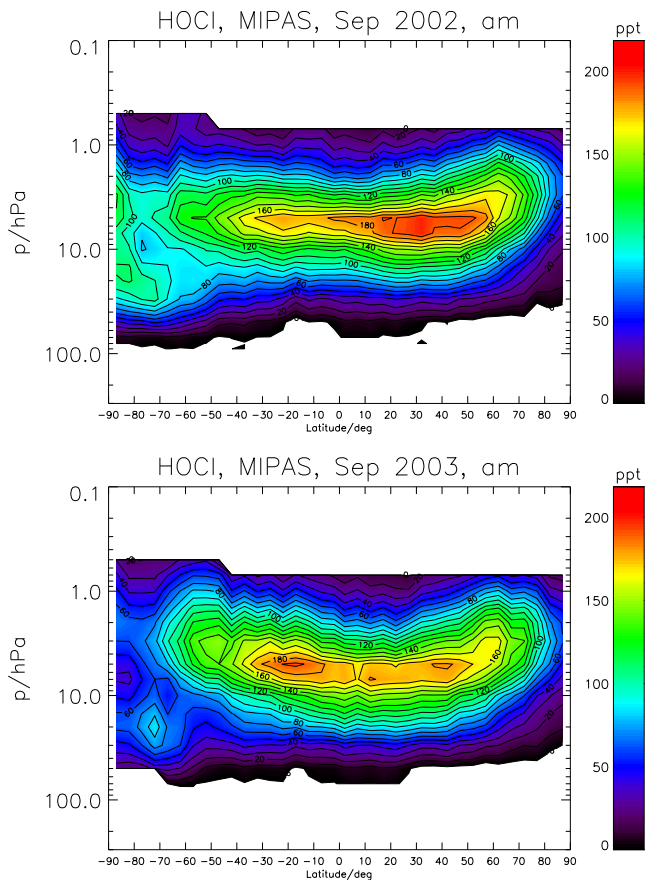


Fig. 8. Large HOCl amounts in the upper southern polar vortex are found in the southern winter 2002 (upper panel) when unusual planetary wave activity led to displacement, deformation, and split of the polar vortex, but not in 2003 (lower panel) when the polar vortex behaved normally. HOCl September zonal mean values of the descending part of the orbit, i.e. morning measurements, are shown.